THE JOURNAL OF BIOLOGICAL CHEMISTRY VOL. 283, NO. 31, pp. 21714–21724, August 1, 2008

Juglone Inactivates Cysteine-rich Proteins Required for Progression through Mitosis*[S]

Received for publication, December 18, 2007, and in revised form, June 4, 2008 Published, JBC Papers in Press, June 6, 2008, DOI 10.1074/jbc.M710264200

Claudia Fila, Corina Metz, and Peter van der Sluijs[1]

From the Department of Cell Biology, University Medical Center Utrecht, AZU G02.525, Heidelberglaan 100, 3584 CX Utrecht, The Netherlands

The parvulin peptidyl-prolyl isomerase Pin1 catalyzes *cis-trans* isomerization of p(S/T)–P bonds and might alter conformation and function of client proteins. Since the *trans* conformation of p(S/T)–P bonds is preferred by protein phosphatase 2A (PP2A), Pin1 may facilitate PP2A-mediated dephosphorylation. Juglone irreversibly inhibits parvulins and is often used to study the function of Pin1 *in vivo*. The drug prevents dephosphorylation of mitotic phosphoproteins, perhaps because they bind Pin1 and are dephosphorylated by PP2A. We show here however that juglone inhibited post-mitotic dephosphorylation and the exit of mitosis, independent of Pin1. This effect involved covalent modification of sulfhydryl groups in proteins essential for metaphase/anaphase transition. Particularly cytoplasmic proteins with a high cysteine content were vulnerable to the drug. Alkylation of sulfhydryl groups altered the conformation of such proteins, as evidenced by the disappearance of antibody epitopes on tubulin and the mitotic checkpoint component BubR1. The latter activates the anaphase-promoting complex/cyclosome, which degrades regulatory proteins, such as cyclin B1 and securins, and is required for mitotic exit. Indeed, juglone-treated cells failed to assemble a mitotic spindle, which correlated with perturbed microtubule dynamics, loss of immunodetectable tubulin, and formation of tubulin aggregates. Juglone also prevented degradation of cyclin B1, independently of the Mps1-controlled mitotic spindle checkpoint. Since juglone affected cell cycle progression at several levels, more specific drugs need to be developed for studies of Pin1 function *in vivo*.

Peptidyl-prolyl isomerases (PPIases)[2] accelerate the *cis-trans* conversion of peptide bonds preceding prolyl residues, which can cause alterations in protein conformation (*e.g.* see Refs. 1 and 2). PPIases have been grouped into cyclophilin, FK506-binding protein, and parvulin subfamilies (see Ref. 3), for which distinct pharmacological inhibitors are available. The parvulin group is irreversibly inhibited by juglone (4). Pin1 comprises an N-terminal type IV WW domain, which determines phosphorylation-specific protein-protein interactions, and a C-terminal PPIase domain that harbors the catalytic center (see Ref. 5). Pin1 is a unique PPIase, because it preferably binds to side chain-phosphorylated S/T-P moieties in numerous proteins, including crucial cell cycle regulators or proteins that become phosphorylated immediately prior to cell division (6, 7). Isomerization of the p(S/T)–P peptide bond regulates, for instance, localization and phosphorylation status of Pin1 client proteins (see Ref. 5). Pin1 is therefore a regulator that, in concert with proline-directed kinases, phosphatases, and ubiquitin ligases, controls the cell cycle (see Refs. 5 and 8). Pin1 is possibly a cancer target gene, because its overexpression enhances transformed phenotypes induced by oncogenic Ras and Neu (see (5)). Pin1 is overexpressed in many human cancers, and its overexpression correlates with poor prognosis of patients (see Ref. 5). For that matter, down-regulation of Pin1 activity by pharmacological agents might present an attractive opportunity for controlling tumor growth. The function of Pin1, however, is more complicated, since loss of Pin1 can cause a selective growth disadvantage, which suggests that Pin1 may have a protective function in oncogenesis of certain cell types (see Ref. 8).

Juglone (5-hydroxy-1,4-naphthalenedione) is a benzoquinone that covalently modifies thiol groups of cysteine residues in parvulin, one of which is essential for PPIase activity (4). It is thought that the inhibition of isomerase activity by juglone is caused by partial unfolding of the PPIase active site (4). Although juglone can inhibit other proteins (9–11), it is frequently used to explore the relevance of Pin1 function *in vivo* (12–14), especially since it often phenocopies effects of Pin1 dominant negative mutants or Pin1 knockdown. For instance, PP2A-mediated dephosphorylation of the Pin1-interacting proteins, Raf-1, Cdc25c, Pim-1, Myc, and Tau, critically relies on Pin1 (15–18). In line with this, juglone prevents the dephosphorylation of MPM2 antigens (19), which constitute a subset of Pin1-interacting mitotic phosphoproteins, as well as of NHERF-1 (20) and Disabled-2 (21). For that matter, it is thought that *cis-trans* isomerization of p(S/T)–P bonds by Pin1 regulates dephosphorylation of PP2A targets by facilitating the accessibility of this phosphatase to its substrates (see Ref. 8).

Several Rab GTPases, including endosomal Rab4a, are phosphorylated by Cdk1 on S/T-P sites within their hypervariable region (22, 23). Rabs are key regulators of membrane traffic (see Ref. 24), and their phosphorylation at the onset of mitosis might

* This work was supported by grants from the Dutch Cancer Society Koningin Wilhelmina Fonds and the Netherlands Organization for Medical Research (to P. v. d. S.). The costs of publication of this article were defrayed in part by the payment of page charges. This article must therefore be hereby marked "*advertisement*" in accordance with 18 U.S.C. Section 1734 solely to indicate this fact.

[S] The on-line version of this article (available at http://www.jbc.org) contains supplemental Figs. S1–S4.

[1] To whom correspondence should be addressed. Tel.: 31-88-7557578; Fax: 31-88-7551797; E-mail: p.vandersluijs@umcutrecht.nl.

[2] The abbreviations used are: PPIase, peptidyl-prolyl isomerase; Rab4a(pS204), phospho-Ser[204]-Rab4a; MEF, mouse embryo fibroblast; PIPES, 1,4-piperazinediethanesulfonic acid; CHO, Chinese hamster ovary; APC/C, anaphase-promoting complex/cyclosome.

be important in the concomitant down-regulation of intracellular transport (22, 23). We previously found that phosphorylated Rab4a binds Pin1 in mitotic cells (25) and that PP2A dephosphorylates Rab4a when cells exit prometaphase.[3] During the analysis of Pin1 function in dephosphorylation of Rab4a, we also employed juglone and made a number of unanticipated observations on the target of the drug. Here we show that treatment of mitotic cells with juglone prevented postmitotic dephosphorylation via pathways that did not involve Pin1. Juglone appears to cause this effect by alkylating sulfhydryl groups in proteins critical for metaphase-anaphase transition, which precludes mitotic exit.

EXPERIMENTAL PROCEDURES

Reagents and Materials—An antibody against phospho-Ser^{204}-Rab4a (Rab4a(pS204)) was raised in rabbits with the keyhole limpet hemocyanin-coupled CRQLRpSPRRTQAPN peptide (where pS represents phosphoserine). Rabbit polyclonal antibodies against human Rab4a and human Pin1 have been described (23, 25). Other antibodies were from the indicated sources: mouse monoclonals MPM2 and BubR1 and rabbit antibodies against the catalytic subunit of PP2A (PP2Ac) and methylated PP2Ac (Upstate Cell Signaling Solutions), mouse monoclonal anti-β-catenin (BD Transduction Laboratories), mouse monoclonal anti-α- and anti-β-tubulin (Sigma), and mouse monoclonal cyclin B1 (Santa Cruz Biotechnology, Inc., Santa Cruz, CA). HRP-labeled and fluorescently labeled secondary antibodies were purchased from Pierce, Jackson Laboratories, and Molecular Probes. Purified protein phosphatase PP2A1 was from Upstate Cell Signaling Solutions, SP600125 was from Sigma, and Alexa488-Annexin V and propidium iodide were from Molecular Probes.

Cell Lines and Synchronization—The CHO-Rab4a cell line (23) and mouse embryonic fibroblasts (MEFs) from Pin1$^{-/-}$ mice (26) were described in the references indicated. Spontaneously immortalized Pin1$^{-/-}$ MEFs were maintained in Dulbecco's modified Eagle's medium supplemented with 10% fetal calf serum, 100 units/ml penicillin, 0.1 mg/ml streptomycin and transfected with pFRSV-Rab4a (23) using calcium phosphate. Clones were selected in the presence of 60 μM methotrexate and were tested for the expression of Rab4a by Western blot. Mitotic CHO and Pin1$^{-/-}$ MEFs were obtained as described (26). In brief, cells were synchronized with 2 mM thymidine. After 15 h, the cells were released from the G_1/S block for 2.5 h and then incubated with 40 ng/ml nocodazole. After 5 h, the cells were harvested by shake-off. U2OS cells were arrested in prometaphase by treatment with 250 ng/ml nocodazole for 18 h.

In Vitro Phosphatase Assay—An *in vitro* assay was used to determine PP2A activity and was conducted as per the vendor's instructions (Molecular Probes). Briefly, 0.2 milliunits of purified PP2A1 was incubated with 6,8-difluoro-4-methyl-umbelliferyl phosphate in 100 μl of phosphatase reaction buffer (50 mM Tris-HCl, pH 7.0, 100 μM $CaCl_2$, 1 mM $NiCl_2$, 100 μg/ml bovine serum albumin, 0.05% Tween 20) containing either juglone or PP2A inhibitors. Reactions were incubated in a microtiter plate in the dark for 1 h at room temperature. Fluorescence was measured in triplicate in a standard fluorescence microtiter plate reader using excitation at 355 nm and emission at 460 nm.

Postmitotic Dephosphorylation Assay—U2OS cells or Rab4-transfected CHO cells and Pin1$^{-/-}$ MEFs were arrested in prometaphase, released from the mitotic block, and incubated in the presence of various concentrations of juglone (with or without 5 mM L-cysteine) for different periods of time. Cell samples were taken and solubilized in lysis buffer (50 mM Tris-HCl, pH 7.5, 150 mM NaCl, 1% Triton X-100, 50 mM NaF, 25 mM β-glycerophosphate, and Roche Complete protease inhibitors). Lysates were cleared by centrifugation at 13,000 rpm in a tabletop centrifuge. Supernatants were collected, and cell pellets were resuspended in an equal volume of 50 mM Tris-HCl, pH 7.5, 150 mM NaCl, 1% SDS. Fractions were equalized for protein content, resolved on 12% SDS-polyacrylamide gels, and analyzed by Western blot.

In Vitro Tubulin Polymerization Assay—Phosphocellulose-purified bovine brain tubulin (>99% purity) was generously provided by Marileen Dogterom (Institute for Atomic and Molecular Physics, Amsterdam) and diluted to 2.2 mg/ml in 80 mM K-PIPES, pH 6.8, 0.5 mM EGTA, 2 mM $MgCl_2$, and 5% glycerol. Tubulin polymerization reactions of 100 μl were prepared in a microtiter plate, and polymerization was started by the addition of 1 mM GTP at 37 °C and followed by A_{340} readings for up to 30 min.

Immunofluorescence Microscopy—Mitotic Pin1$^{-/-}$ MEFs were seeded on poly-L-lysine-coated coverslips and incubated for up to 60 min in the presence of 1 μM juglone. Cells were fixed in ice-cold methanol and subsequently processed for indirect immunofluorescence microscopy. Cells were labeled for α-tubulin and stained with Alexa488-conjugated anti-mouse IgG. DNA was visualized with 4′,6-diamidino-2-phenylindole. Coverslips were mounted and dried, and cells were viewed with a Zeiss LSM5 confocal microscope.

Flow Cytometry—Interphase CHO cells were treated with increasing concentrations of juglone for 180 min. Cells were harvested, washed in phosphate-buffered saline, and resuspended at a density of ~1×10^6 cells/ml in 10 mM Hepes, pH 7.4, 140 mM NaCl, and 2.5 mM $CaCl_2$. Alexa488-Annexin V and propidium iodide were added for 15 min at room temperature according to the manufacturer's instructions. Samples were immediately analyzed on a FACSVantage SE cell sorter (Becton Dickinson) using the 488-nm laser. Results were quantitated in Cellquest. Pin1$^{-/-}$ MEFs were treated for 15 h with increasing concentrations of juglone. During the last hour, Hoechst 33342 (10 μg/ml) was added to stain DNA. Cells were trypsinized, and cell cycle profiles were obtained by cytometric analysis on a FACSVantage SE cell sorter using the UV laser. The number of cells in different cell cycle phases (M_1–M_4) was evaluated in Cellquest.

RESULTS

Rab4a is phosphorylated during mitosis by Cdk1 on Ser^{204} (23) and dephosphorylated by PP2A when cells exit prometaphase.[4] We here employed the parvulin PPIase inhibitor

[3] C. Fila and P. van der Sluijs, unpublished results.

[4] C. Fila and P. van der Sluijs, manuscript in preparation.

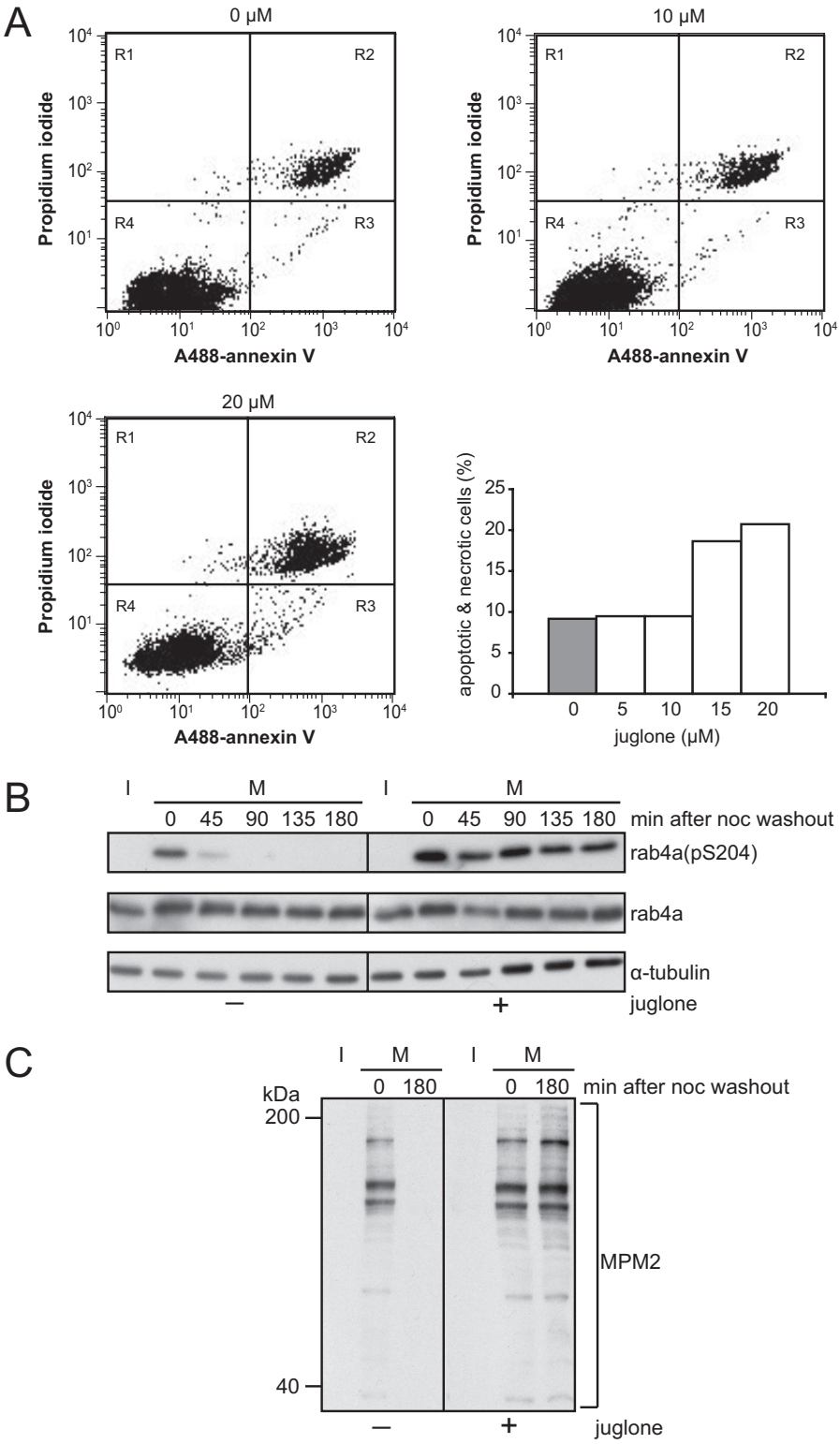

FIGURE 1. **Juglone inhibits postmitotic dephosphorylation of Rab4a.** *A*, interphase CHO cells were treated for 3 h with increasing concentrations of juglone. Binding of Alexa488-annexin V (A488-annexin V) and permeability to propidium iodide was analyzed by fluorescence-activated cell sorting. Density dot plots were used to quantitate the ratio apoptotic/Annexin V-positive (*R2* and *R3*) and dead/propidium iodide-positive (*R1* and *R2*) as presented in the *bar diagram*. *B*, Interphase (*I*) and mitotic (*M*) CHO-Rab4a transfectants were incubated with 7.5 μM juglone (+) or solvent (−). Lysates were prepared at the indicated periods of time after nocodazole (*noc*) washout and were analyzed by Western blot with antibodies against Rab4a(pS204) and Rab4a. α-Tubulin served as loading control. *C*, MPM2 antigens were detected in detergent lysates of juglone-treated interphase as well as mitotic cells taken 0 and 180 min after nocodazole washout.

juglone initially, to analyze a possible role of Pin1 in the dephosphorylation of Ser^{204}.

Juglone Titration on CHO Cells—Because high concentrations of juglone affect cell viability (27, 28), we performed a titration study to establish an optimal concentration of the inhibitor. CHO cells were incubated with increasing concentrations of juglone and stained with Alexa488-Annexin V to assess the extent of apoptosis and with propidium iodide to distinguish between living and dead cells by fluorescence-activated cell sorting analysis. As shown in the *bar diagram* in Fig. 1*A*, less than 10 μM juglone did not cause apoptosis (*R2* and *R3*) or necrosis (*R1* and *R2*), compared with controls. Concentrations above 10 μM increased the number of both apoptotic and necrotic cells. Most of the Annexin V-labeled cells were also positive for propidium iodide, showing that the majority had already entered late stages of apoptosis. In the subsequent *in vivo* experiments in CHO cells, we used 7.5 μM juglone, since this concentration did not induce apoptosis or cell death and is close to the minimal concentration that inactivates parvulins *in vitro* (4).

Juglone Prevents Postmitotic Dephosphorylation of Rab4a—Mitotic CHO-Rab4a cells were released from prometaphase arrest and incubated in the presence of 7.5 μM juglone. Nonsynchronized (interphase) cells were treated the same and served as negative control. Timed samples were analyzed by Western blot with an antibody against phosphorylated Ser^{204} in Rab4a. Within 45 min after release of the mitotic block, more than 90% of Rab4a was dephosphorylated in control cells as shown in Fig. 1*B*. In contrast, Rab4a remained fully phosphorylated in the presence of juglone. Samples were also probed with the MPM2 antibody, which recognizes a multitude of proteins containing phosphorylated S/T-P sites with a molecular mass between ~35 and 300 kDa (29).

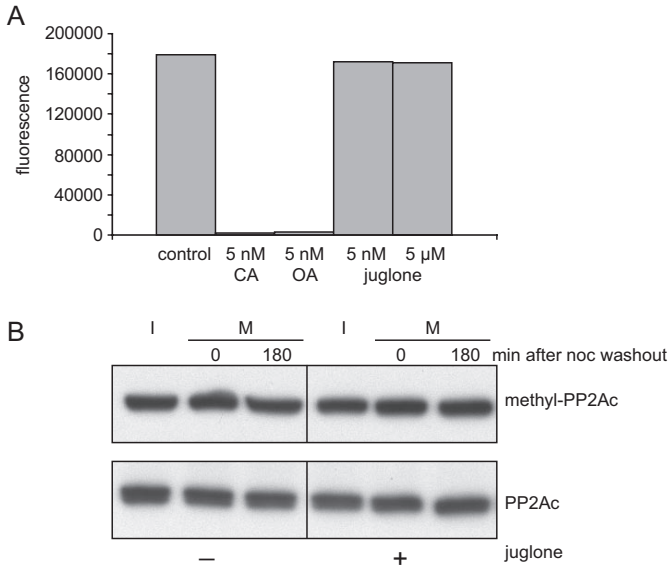

FIGURE 2. **Juglone does not affect PP2A activity.** *A*, *in vitro* assay for PP2A1-dependent dephosphorylation of 6,8-difluoro-4-methyl-umbelliferyl phosphate in the presence of juglone or the Ser/Thr phosphatase inhibitors calyculin A (*CA*) and okadaic acid (*OA*). *B*, lysates of interphase (*I*) and mitotic (*M*) CHO cells were probed with antibodies against the catalytic (PP2Ac) subunit of PP2A and the methylated form of the enzyme (methyl-PP2Ac). *noc*, nocodazole.

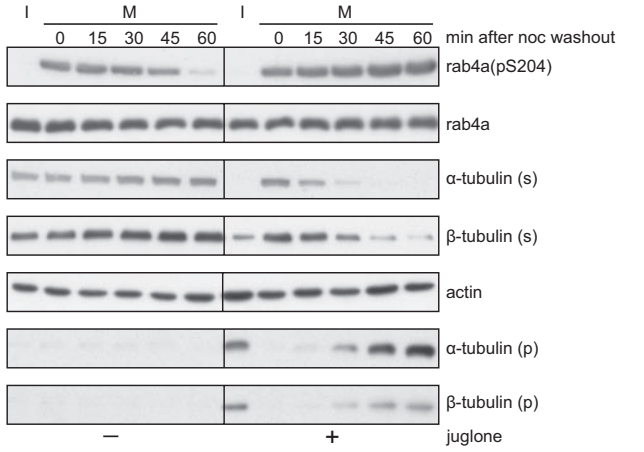

FIGURE 3. **Juglone inhibits postmitotic dephosphorylation in the absence of Pin1.** Interphase (*I*) and mitotic (*M*) Pin1$^{-/-}$ MEFs expressing Rab4a were incubated with 7.5 μM juglone or solvent (−) for up to 60 min. Cells were lysed at the indicated times after nocodazole washout, and cleared extracts (soluble fraction (*s*)) were detected for pSer204-Rab4a, Rab4a, α-tubulin, β-tubulin, and actin by Western blotting. Insoluble cell pellets (*p*) were extracted with Laemmli sample buffer, resolved under reducing conditions, and analyzed for α- and β-tubulin by Western blotting.

The entire set of MPM2 antigens was dephosphorylated after 180 min of nocodazole washout in control cells (Fig. 1*C*). In the juglone-treated cells, MPM2 staining remained at the initial level. We therefore concluded that juglone prevented dephosphorylation of mitotic phosphoproteins, including Rab4a. Similar results were reported for Disabled-2, NHERF-1, and MPM2 antigens and proposed to be caused by inhibition of PP2A-mediated dephosphorylation due to loss of Pin1 function (19–21).

Juglone Does Not Inhibit PP2A—PP2A is a heterotrimer consisting of a scaffolding (A), a regulatory (B), and a catalytic (C) subunit (30). Since juglone is known to inhibit proteins other than just parvulins (9–11), and since naphtoquinones inactivate protein-tyrosine phosphatases (31), we first investigated the possibility that juglone might act directly on PP2A. We therefore measured the activity of purified heterotrimeric PP2A1 in the presence of juglone in an *in vitro* assay. The assay measures dephosphorylation of the Ser/Thr phosphatase substrate 6,8-difluoro-4-methyl-umbelliferyl phosphate, which generates fluorescent 6,8-difluoro-4-methyl-umbelliferyl with excitation/emission maxima at 358/452 nm. Whereas established PP2A inhibitors calyculin A and okadaic acid reduced the fluorescence intensity more than 95% with respect to control levels, juglone did not affect PP2A as shown in Fig. 2*A*. Since maximal activity of PP2A *in vivo* requires methylation of the C subunit (30), we also analyzed in cells whether juglone affected this posttranslational modification. As shown in Fig. 2*B*, juglone did not inhibit PP2A methylation, as we found by Western blot with a specific antibody against the methylated form of the C subunit of PP2A. Collectively, the assays for PP2A activity and PP2A methylation showed that juglone did not inhibit PP2A directly and that postmitotic dephosphorylation of Rab4a is unlikely to be due to inhibition of the phosphatase.

Juglone Blocks Postmitotic Dephosphorylation in Pin1$^{-/-}$ Cells—Having shown that inhibited dephosphorylation of mitotic phosphoproteins (Fig. 1, *B* and *C*) is not caused by a direct effect of juglone on PP2A (Fig. 2, *A* and *B*), we next investigated whether the block was due to inhibition of Pin1. For that matter, we studied dephosphorylation of mitotically phosphorylated Rab4a in MEFs derived from Pin1$^{-/-}$ mice (26). The cells lacked immunologically detectable Pin1, as evidenced by a Western blot with a polyclonal antibody against Pin1 (Fig. S1). As a consequence of Pin1 deficiency, the cells also contained ~40% less of the Pin1 client protein β-catenin (Fig. S1), whose stability correlates directly with Pin1 expression levels (32). The reduced β-catenin levels in Pin1$^{-/-}$ MEFs also suggested that the cells do not have salvage mechanisms to counteract the loss of Pin1 activity. Pin1$^{-/-}$ MEFs were next released from the mitotic block and incubated in the presence of 7.5 μM juglone for up to 60 min. The cells were then harvested at different periods of time after nocodazole washout, and detergent lysates were analyzed for the amounts of Rab4a(pS204) and total Rab4a. The rate of Rab4a dephosphorylation in the absence of Pin1 was comparable with that in CHO cells (Fig. 3). Even in a genetic model for the loss of Pin1 function, juglone inhibited the dephosphorylation of Rab4a in the Pin1$^{-/-}$ MEFs (Fig. 3). These results showed that the effect of juglone is not caused by a mechanism involving Pin1.

Juglone Decreased Tubulin Content in Lysates—Careful analysis of the experiments with the Pin1$^{-/-}$ cells revealed an additional effect of juglone treatment. We found that the amount of α- and β-tubulin decreased during the release of the mitotic block in the presence of juglone (Fig. 3). This observation was also made in interphase cells that were treated for 60 min with juglone, documenting that the cell cycle stage was immaterial to this effect of the drug. The disappearance of α- and β-tubulin was not caused by leakage of cytosolic proteins, because actin levels remained the same throughout the experiment. To account for the loss of α- and β-tubulin from the detergent

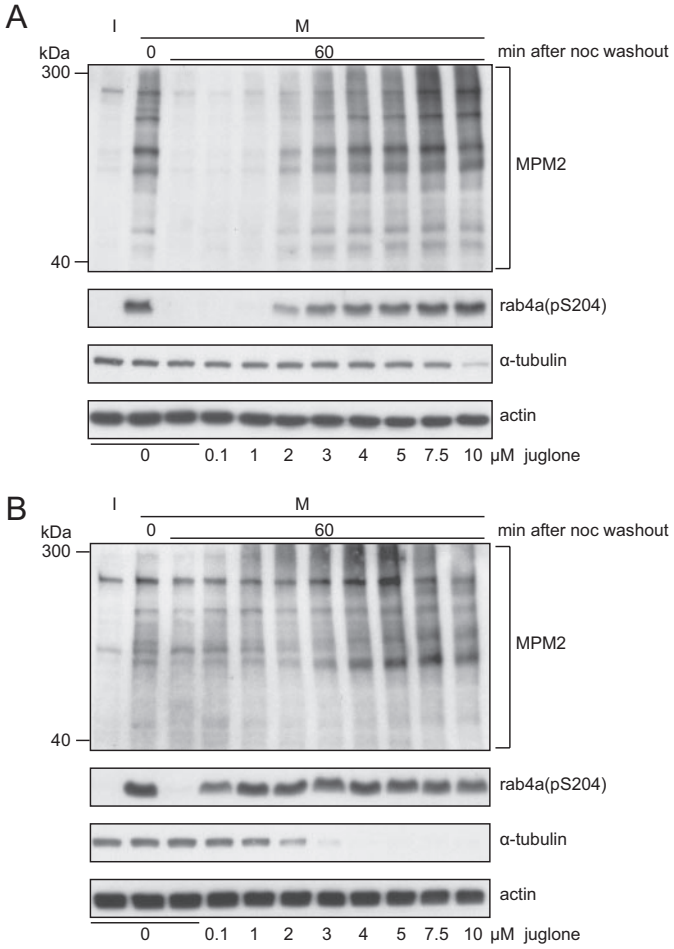

FIGURE 4. **Juglone causes tubulin aggregation.** CHO cells (*A*) or Pin1$^{-/-}$ MEFs (*B*) were released from mitotic arrest by washout of nocodazole (*noc*) and incubated for 60 min with increasing amounts of juglone. Lysates of nontreated interphase (*I*) and mitotic (*M*) cells and mitotic cells treated with juglone were analyzed for Rab4a(pS204), α-tubulin, actin, and MPM2 antigens.

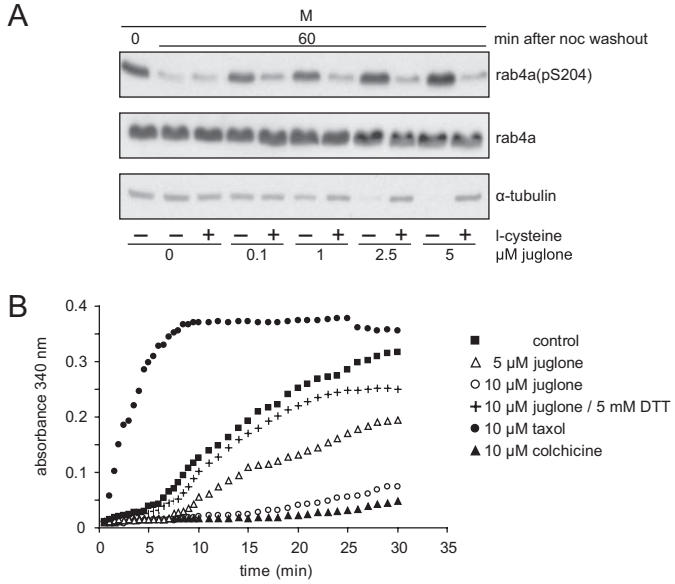

FIGURE 5. **Role of SH groups in tubulin aggregation.** *A*, Pin1$^{-/-}$ MEFs were released from mitotic block in nocodazole (*noc*)-free medium and were incubated with increasing amounts of juglone in the presence of L-cysteine. Lysates were analyzed for Rab4a(pS204), Rab4a, and α-tubulin by Western blotting. *B*, polymerization of phosphocellulose-purified brain tubulin in the presence of the indicated reagents was assayed by measuring dynamic light scattering at 340 nm.

lysates, we evaluated whether the tubulins were sedimented in the Triton X-100-insoluble pellet that was generated during preparation of cleared lysates. Pellets were solubilized in reducing Laemmli buffer and analyzed by Western blot. As shown in Fig. 3, the amount of Triton X-100-insoluble (from now on called insoluble) α- and β-tubulin increased in a time-dependent manner in the presence of juglone. Insoluble, presumably aggregated α- and β-tubulin was also detected in the pelleted material of juglone-treated interphase cells (Fig. 3). Thus, juglone rendered tubulin partially insoluble in Pin1$^{-/-}$ MEFs.

Although 7.5 μM juglone caused aggregation of tubulin in Pin1$^{-/-}$ MEFs, we did not observe this in CHO cells (Fig. 1*B*). To investigate whether or not the effect on the Triton X-100 solubility of tubulin (from now on called solubility) was restricted to Pin1$^{-/-}$ MEFs, we performed juglone titrations on CHO cells and Pin1$^{-/-}$ MEFs. Nocodazole-arrested mitotic cells were harvested and incubated for 60 min in medium containing increasing juglone concentrations. Cell lysates were then analyzed for Rab4a(pS204), MPM2 antigens, α-tubulin, and actin. As shown in Fig. 4*A*, juglone concentrations above 2 μM inhibited dephosphorylation of Rab4a and MPM2 antigens in CHO cells. The amount of soluble α-tubulin only started to decrease at juglone concentrations above 10 μM. The initial experiments with CHO cells in which we found inhibited postmitotic dephosphorylation (Fig. 1*B*) were done with 7.5 μM, which did not affect tubulin solubility (Fig. 4*A*). In Pin1$^{-/-}$ MEFs, the dephosphorylation of phospho-Rab4a was already inhibited by as little as 0.1 μM juglone (Fig. 4*B*), whereas tubulin became insoluble at juglone concentrations above 2 μM (Fig. 4*B*). Thus, the dose-dependent effects of the Pin1 inhibitor on dephosphorylation of mitotic phosphoproteins and tubulins were not limited to Pin1$^{-/-}$ MEFs but were also recapitulated in another cell line. The experiments in Figs. 2 and 4 also showed that dephosphorylation of mitotic phosphoproteins is a more sensitive read-out than the generation of insoluble tubulin.

Juglone Affects Tubulin Function via Alkylation of SH Groups—Juglone can covalently modify free SH groups of cysteine residues, which is the basis for the inactivation of Pin1 (4) and probably of other proteins (33). To examine if the effects of juglone on tubulin and dephosphorylation of mitotic phosphoproteins are caused by such reactivity, we incubated mitotic Pin1$^{-/-}$ MEFs with increasing concentrations of juglone in the absence or presence of an excess of L-cysteine. In agreement with the results of Fig. 4*B*, the postmitotic dephosphorylation of Rab4a was inhibited at concentrations above 0.1 μM, and the aggregation of tubulin became detectable above 2.5 μM juglone. The addition of L-cysteine essentially reversed the effects of juglone (Fig. 5*A*). Thus, L-cysteine protected the cells from juglone-induced tubulin aggregation and the concomitant block of mitotic exit. The protective function of L-cysteine strongly indicates that juglone-mediated tubulin aggregation is due to the direct modification of one or more of the 21 cysteines of the αβ-tubulin dimer (34).

The modification and aggregation of tubulin will probably affect its incorporation into microtubules. We therefore performed *in vitro* polymerization reactions with phosphocellulose-purified brain tubulin to investigate whether or not juglone directly interfered with the assembly of tubulin into microtubules. Highly purified bovine brain tubulin, devoid of microtubule-associated proteins, was resuspended in PIPES buffer in the presence of different concentrations of juglone. Reactions with taxol and colchicine served as controls, since they either stimulate or inhibit tubulin polymerization, respectively (35). As shown in Fig. 5*B*, 5 μM juglone reduced tubulin polymerization to about 60%, and 10 μM blocked it to nearly the same extent as colchicine. The addition of 5 mM DTT to the reaction containing 10 μM juglone rescued tubulin polymerization and restored it to ~80%. Taken together, these data showed that juglone acted directly on tubulin and inhibited tubulin polymerization through modification of its SH groups.

Given the effects of juglone on tubulin solubility *in vivo* and the assembly of tubulin polymers, we determined whether microtubule organization is affected by the drug. Pin1$^{-/-}$ MEFs and CHO cells were incubated for 120 min with different concentrations of juglone. Cells were then fixed and labeled for α-tubulin. Low concentrations of juglone that prevented postmitotic dephosphorylation of Rab4a but did not induce overt tubulin aggregation (1 μM for MEFs and 5 μM for CHO cells) also did not affect the morphology of the microtubule networks in both cell lines (Fig. S2*A*). Juglone concentrations that cause clear immunodetectable aggregation of tubulin (5 μM for MEFs and 15 μM for CHO) essentially resulted in the complete disassembly of microtubule networks, and a shift toward cytosolic tubulin staining similar to what is seen when cells were treated with the microtubule-depolymerizing drug colchicine (Fig. S2*A*). Since low concentrations of juglone did not affect morphological integrity of microtubule networks in interphase CHO cells and Pin1$^{-/-}$ MEFs, we extended the incubation period with low juglone concentrations to 12 h and assessed the effect on tubulin solubility in a sedimentation assay. Colchicine was included as control, since it depolymerizes microtubules. Cells were lysed, and α-tubulin was then analyzed by Western blotting of the Triton X-100-soluble/insoluble fractions. In order to detect aggregated α-tubulin in the detergent-insoluble fraction, we loaded 5 times more of this fraction than of the soluble pool. The amount of pelleted α-tubulin increased 2.5-fold in the presence of 1 μM juglone compared with nontreated control cells (Fig. S2*B*). In the presence of 10 μM juglone, the entire pool of soluble α-tubulin was aggregated (not shown). Although there was clearly a dose-dependent increase in the amount of pelleted α-tubulin, this represented a relatively modest fraction compared with the total pool. In colchicine-treated cells, α-tubulin was only detectable in the supernatant, as might be expected given its microtubule-depolymerizing effect. Polymerized $\alpha\beta$-tubulin in microtubules is in dynamic equilibrium with a soluble pool. Alterations in the concentration of soluble tubulin will therefore affect the equilibrium and indirectly the integrity of microtubules. In addition, it is likely that the small molecule inhibitor will also affect microtubules directly by modifying surface-exposed cysteines in microtubule-tubulin.

Juglone Does Not Arrest Cells in Metaphase—Because juglone treatment disrupted microtubule networks, we also evaluated whether juglone can arrest asynchronously growing cells in metaphase. To this aim, Pin1$^{-/-}$ MEFs were treated for 12 h with different concentrations of the drug, and the appearance of the mitotic marker protein phospho-Rab4a was determined. As controls, we included taxol, nocodazole, and colchicine, which arrest cells in mitosis (35). Unlike the three spindle poisons, juglone treatment of interphase cells failed to generate the Rab4a(pS204) epitope in Pin1$^{-/-}$ MEFs (Fig. 6*A*) and CHO cells (not shown). The cells were next investigated by flow cytometry to evaluate potential juglone-mediated effects on DNA content. Histograms of cell populations treated with increasing juglone concentrations are shown in Fig. 6*B*. Up to 5 μM juglone caused a gradual decrease of cells in G_2/M phase (M_3) and a concomitant increase in the number of cells residing in S phase (M_2), (Fig. 6*B*, *table*). Higher concentrations also reduced the number of cells in S phase with an accompanying increase of cells with sub-G_1 DNA content (M_4) (Fig. 6*B*, *table*). Thus, low juglone concentrations arrested cells in particular stages of their life cycle, whereas high doses of the drug or long term treatment induce cells to undergo apoptosis. Similar results were obtained with CHO cells that were first synchronized at the G_1/S boundary by thymidine and then released into S phase for 2.5 h and finally treated with 7.5 μM juglone for 6 h. Whereas the same treatment with nocodazole allowed for the generation of robust signals of Rab4a(pS204) and MPM2 antigens (Fig. S3*A*) as well as a significant increase of cells with 4 N DNA content (Fig S3*B*, *table*), juglone failed to arrest cells efficiently in prometaphase of mitosis. Thus, although juglone and colchicine both disrupted microtubules (Fig. S2), the different sedimentation characteristics of tubulin (Fig. S2*B*) and the inability of juglone to block cells in metaphase (Fig. 6 and Fig. S3) showed that the two drugs interfere with microtubule function in a distinct manner.

Juglone Inhibits Mitotic Spindle Assembly—Short term treatment with low doses of juglone did not disrupt interphase microtubule networks (Fig. 4*C*). Such concentrations might however disturb microtubule polymerization under conditions that require higher microtubule dynamics and increased tubulin turnover. For instance, at the onset of mitosis, the catastrophe rate of microtubules changes, because assembly of the mitotic spindle requires shorter and more dynamic microtubules (36). Highly dynamic microtubules might be more susceptible toward reagents that cause subtle alterations in structure and function of tubulin. To pursue this idea, we investigated microtubule rearrangements in Pin1$^{-/-}$ MEFs during exit from mitosis. Pin1$^{-/-}$ MEFs were arrested in prometaphase, released from the mitotic block, and seeded on poly-L-lysine-coated coverslips in the presence of 1 μM juglone. Cells were fixed after different periods of time and labeled for α-tubulin, and DNA was stained with 4′,6-diamidino-2-phenylindole. Control cells that were released from the prometaphase block passed through mitosis, as visualized by the ordered appearance of characteristic mitotic profiles (Fig. 7*A* and Fig. S4, *left column*). Initially, the cells contained clearly condensed chromatin and predominantly nonpolymerized tubulin. After 15 min, most of the cells established a spindle

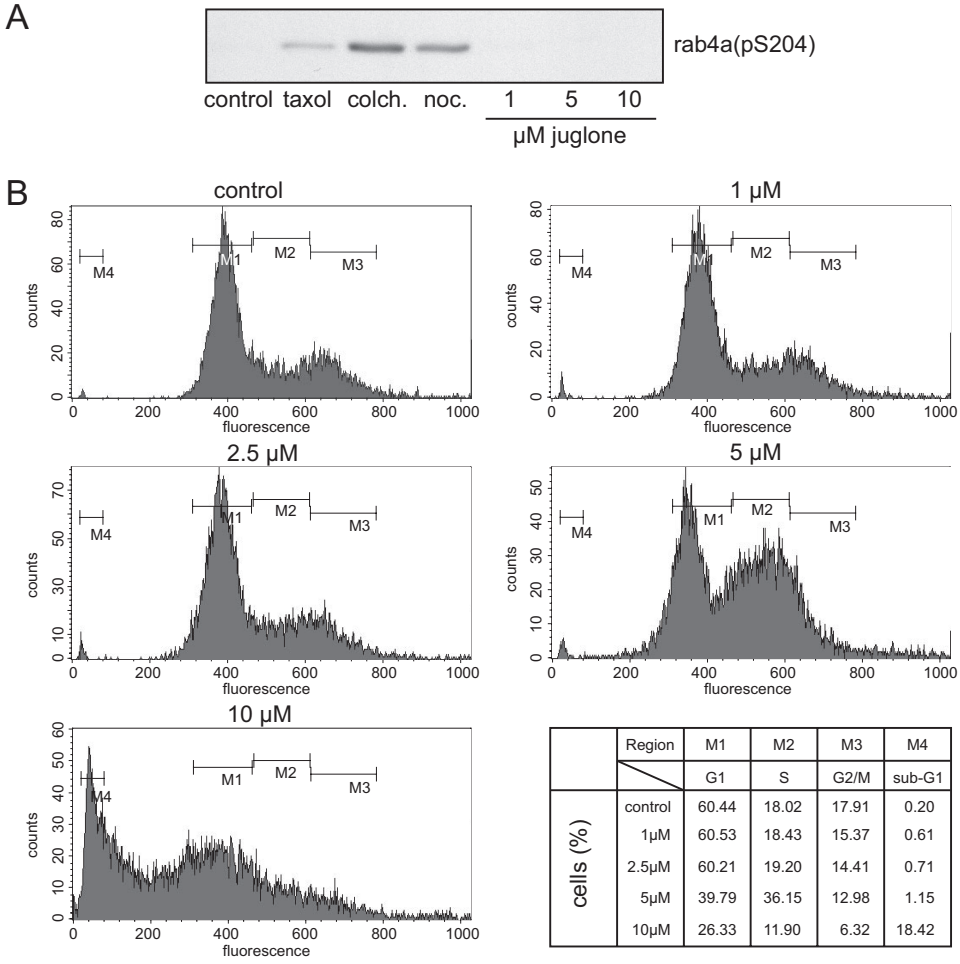

	Region	M1	M2	M3	M4
		G1	S	G2/M	sub-G1
cells (%)	control	60.44	18.02	17.91	0.20
	1μM	60.53	18.43	15.37	0.61
	2.5μM	60.21	19.20	14.41	0.71
	5μM	39.79	36.15	12.98	1.15
	10μM	26.33	11.90	6.32	18.42

FIGURE 6. **Juglone does not arrest cells in mitosis.** *A*, interphase Pin1$^{-/-}$ MEFs were treated for 12 h with juglone, taxol, colchicine (*colch.*), or nocodazole (*noc*). Cells were lysed, and Rab4a(pS204) was determined by Western blotting. *B*, interphase Pin1$^{-/-}$ MEFs were treated with different concentrations of juglone for 15 h. DNA was stained with Hoechst 33342 for 1 h, and cell cycle profiles were obtained by flow-cytometric analysis. The percentages of cells in the different cell cycle phases (M_1–M_4) are quantitated and represented in a *table*.

apparatus, and chromosomes were aligned in the metaphase plate. After 30 min, cells were in the process of being pulled toward opposite spindle poles and thus had passed the metaphase/anaphase transition. After 60 min, almost all cells displayed early or late stages of cytokinesis; some had already flattened and reestablished a typical interphase microtubule network. In contrast, cells that were treated with juglone (Fig. 7*A* and Fig. S4, *right column*) retained a tubulin staining pattern that is typical for prometaphase (*cf.* time 0) and failed to assemble a mitotic spindle or align chromosomes in the metaphase plate. In agreement with these results, the mitotic index, as quantitated using 4′,6-diamidino-2-phenylindole staining of condensed chromatin (Fig. S4) or with phosphohistone 3 labeling (not shown), remained constant at ~90% during juglone treatment. Identical results were found in CHO cells treated with 5 μM juglone (not shown). This suggested that juglone precludes the formation of a mitotic spindle at concentrations that blocked postmitotic dephosphorylation but did not yet cause detectable tubulin aggregation and collapse of interphase microtubules. Thus, cellular events that require a highly dynamic microtubule cytoskeleton were more sensitive toward juglone than interphase microtubules.

Juglone Prevents Degradation of Cyclin B1—As a consequence of compromised spindle assembly or damage, the mitotic spindle checkpoint becomes activated. A series of tightly controlled reactions is then initiated, which prevents activation of the anaphase-promoting complex/cyclosome (APC/C) and proteasomal destruction of anaphase inhibitors, such as cyclin B1, which is the critical event permitting mitotic exit (see Ref. 37). Given the impact of juglone on spindle assembly, we next investigated its effect on cyclin B1 levels as read-out for the potential activation of the mitotic spindle assembly checkpoint. Mitotic and interphase Pin1$^{-/-}$ MEFs were incubated for 120 min with 1 μM juglone. Juglone-treated cells and control cells were lysed and analyzed for cyclin B1 by Western blotting. When cells were released from the mitotic block in the presence of juglone, degradation of cyclin B1 was prevented. Cyclin B1 levels at 120 min after nocodazole washout were identical to those at time 0 (Fig. 7*B*). In contrast, 2 h after nocodazole washout, when Pin1$^{-/-}$ MEFs are known to have exited mitosis (Fig. 7*A*), cyclin B1 was degraded in control cells to a similar level as present in interphase cells (Fig. 7*B*). Evidently, juglone prevented the degradation of cyclin B1, the essential cofactor of Cdk1. This might explain the inhibition of postmitotic protein dephosphorylation in the presence of juglone, since as long as Cdk1 is active, it will keep on phosphorylating its targets.

Juglone Prevents Postmitotic Protein Dephosphorylation in the Absence of Active Spindle Checkpoint Factors—To investigate a direct role of the mitotic spindle checkpoint in the abolished degradation of cyclin B1 and the inhibited dephosphorylation of mitotic phosphoproteins, we examined the activity of spindle checkpoint factors in juglone-treated cells. These represent regulators of the Mad and Bub families (see Ref. 37). In the case of spindle damage or a lack of tension on spindle microtubules, they are activated and recruited to the kinetochore region of the chromatids. The serine/threonine kinase Mps1 (monopolar spindle 1) is an essential upstream regulator whose activity is essential for the initiation of the checkpoint signaling cascade (38) through phosphorylation of other checkpoint proteins, such as Mad2 and Bub1 (see Ref. 37). We treated mitotic Pin1$^{-/-}$ MEFs and U2OS cells with either nocodazole or juglone and 10 μM SP600125, a known Mps1 inhibitor (39). The inhibition of Mps1 kinase would allow cells to override the spindle checkpoint and to dephosphorylate mitotic proteins

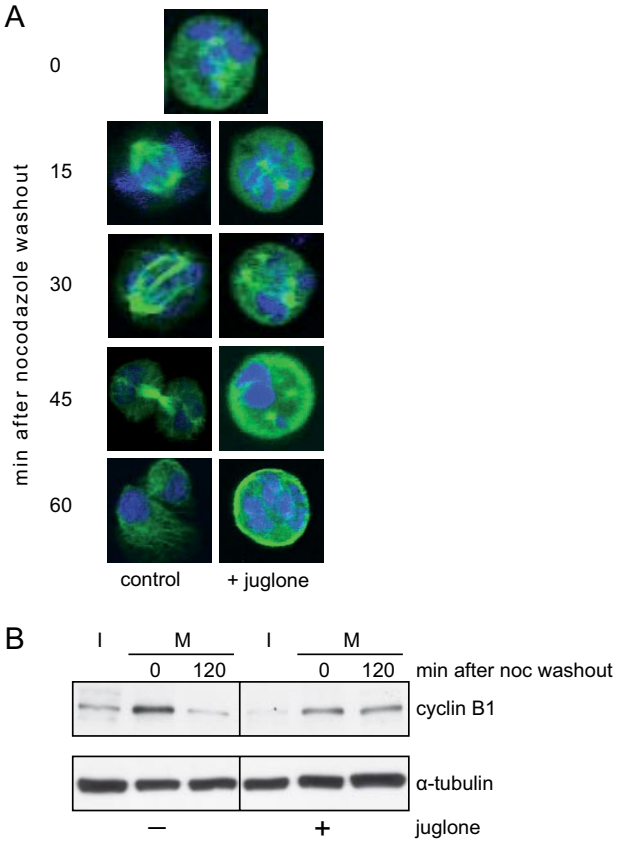

FIGURE 7. **Juglone inhibits mitotic spindle formation.** *A*, Pin1$^{-/-}$ MEFs were released from mitotic arrest by removal of nocodazole (*noc*) and reseeded on coverslips. Cells were incubated with 1 μM juglone and fixed at the indicated times after nocodazole washout. Cells were labeled for α-tubulin (*green*), stained for DNA (*blue*), and examined by fluorescence microscopy. *Images* are *enlargements* of the *insets* from Fig. S4*A* show a mitotic figure representative for the majority of cells at this time point. *B*, interphase (*I*) and mitotic (*M*) cells after nocodazole washout were incubated with 1 μM juglone for 120 min and analyzed for cyclin B1 and α-tubulin by Western blotting.

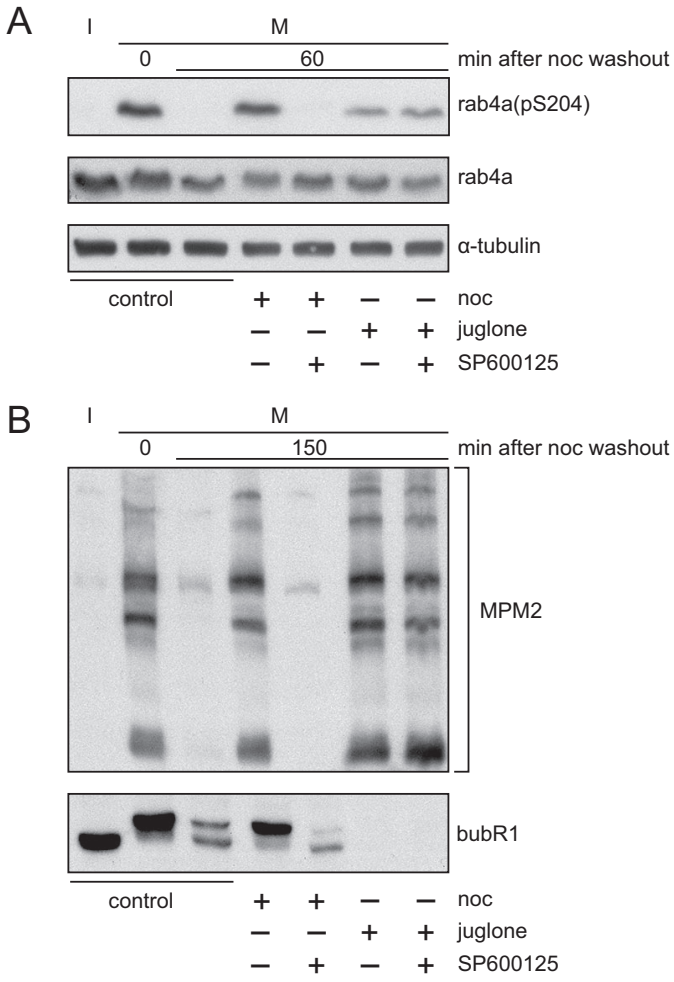

FIGURE 8. **Juglone prevents postmitotic protein dephosphorylation in the absence of an active spindle checkpoint.** *A*, mitotic Pin1$^{-/-}$ MEFs were incubated for 1 h either without drugs (control) or with the indicated combinations of drugs: nocodazole (*noc*) (40 ng/ml), juglone (1 μM), and SP600125 (10 μM) SP600125. Detergent lysates were analyzed for phospho-Rab4a, Rab4a, and α-tubulin by Western blotting. *B*, mitotic U2OS cells were incubated for 2.5 h with a similar drug regimen as in *A*. Concentrations of the drugs were adapted to this cell type and were nocodazole (250 ng/ml), juglone (5 μM), and SP600125 (10 μM). MPM2 antigens and BubR1 were assayed by Western blot of detergent lysates.

also in the presence of a spindle poison (*i.e.* in the absence of a functional mitotic spindle) (39). As shown in Fig. 8, *A* and *B*, nocodazole maintained Pin1$^{-/-}$ MEFs and U2OS cells in prometaphase, as evidenced by the Rab4a(pSer204) and MPM2 signals, respectively. When we added SP600125 in combination with the spindle poison, both Rab4a(pS204) (Fig. 8*A*) and MPM2 antigens (Fig. 8*B*) were dephosphorylated. When we repeated the experiment with juglone instead of nocodazole, SP600125, surprisingly, did not affect the phosphorylation status of mitotic phosphoproteins, since neither Rab4a nor MPM2 antigens (Fig. 8*B*) became dephosphorylated.

We also analyzed U2OS cell lysates for the essential spindle checkpoint kinase BubR1. It is extensively phosphorylated by Cdk1 and Polo-like kinase 1 during mitosis (40), which is easily visualized by a mobility shift on SDS-polyacrylamide gels, as shown in Fig. 8*B*. The addition of SP600125 clearly diminished the mobility shift of BubR1 in cells that were treated with nocodazole. The effect of SP600125 is due to inhibition of Mps1 and the inactivation of the checkpoint and reflects the rapid dephosphorylation of BubR1. We then analyzed the expression of BubR1 in U2OS cells that were treated with juglone. As shown in the Western blot of Fig. 8*B*, BubR1 was not detectable anymore, irrespective of whether SP600125 was present or not. BubR1 is a cytoplasmic protein containing 21 cysteine residues, of which the SH groups are expected to be in the free form. This represented a similar situation as tubulin with its high cysteine content, suggesting that juglone also covalently modified the free thiol groups of BubR1 and affected its folding in a normal functional state. Since the extent of MPM2 staining is the same in juglone-treated and mitotic control U2OS cells (Fig. 8*B*), the absence of BubR1 was not caused by apoptosis or cell leakage. Taken together, our data strongly suggest that juglone acts directly on cysteine-rich proteins, such as tubulin, which appears to interfere with their normal function. Interestingly, although juglone maintained high levels of cyclin B1 and strongly affected spindle assembly, it precluded mitotic exit without the direct involvement of the mitotic spindle checkpoint.

DISCUSSION

We investigated a possible role of Pin1 in the dephosphorylation of mitotic phosphoproteins by PP2A at the end of mitosis. We initially focused on Rab4a, since it is targeted by Cdk1, in complex with Pin1 during mitosis (25), and dephosphorylated when cells exit M phase. In experiments with the Pin1 inhibitor juglone, we found that dephosphorylation of Rab4a and of MPM2 antigens was strongly reduced. Previously, it was shown that juglone inhibits dephosphorylation of Pin1-interacting mitotic phosphoproteins, such as NHERF-1 and Disabled-2, a phenotype that was thought to represent a specific effect of Pin1 inhibition (18–21). This paradigm was largely built on studies in which Pin1 client proteins required the isomerase for dephosphorylation by PP2A during interphase (15–17).

Juglone is a naphthoquinone, a class of organic compounds whose biological effects are largely caused by the formation of reactive oxygen species through redox activation and the covalent modification of free thiols to form thioethers (see Refs. 41 and 42)). To avoid cell death through apoptosis or necrosis during our experiments, we first conducted juglone titration studies with CHO cells to establish an optimal concentration. Therefore, the juglone concentrations used in our study were orders of magnitude below those often used in earlier studies aimed at inhibiting Pin1 *in vivo* (12–14, 27). Moreover we treated the cells only for relatively short periods of time with the drug.

Our results clearly showed that juglone-mediated inhibition of mitotic phosphoprotein dephosphorylation (MPM2 antigens) at the end of mitosis is not caused by inhibition of Pin1. Likewise, the drug did not inactivate PP2A or factors involved in the methylation of the catalytic subunit of PP2A. Instead, juglone inhibited the dynamics of microtubules and prohibited the assembly of a mitotic spindle at concentrations that did not cause apoptosis or necrosis. These *in vivo* findings are consistent with the reported covalent binding of *p*-benzoquinone derivatives to tubulin *in vitro* (43, 44).

The lowest juglone concentrations that prevented mitotic exit, however, left the microtubule networks in interphase cells untouched. This strongly suggested that mitotic microtubules are more sensitive toward juglone. Indeed, at the onset of mitosis, the array of long and stable microtubules is replaced by a set of short and fragile microtubules with a faster tubulin turnover (45). This architectural editing is necessary for spindle formation and chromosome segregation (36). In addition to the complete inhibition of mitotic spindle formation or the alignment of chromosomes in the metaphase plate, juglone also inhibited destruction of cyclin B1, the essential cofactor of Cdk1. Both observations suggested that the compromised mitotic exit might be a result of the activation or maintenance of the mitotic spindle checkpoint. However, this idea is not tenable given the data obtained with the Mps1 inhibitor SP600125. If juglone were to maintain the mitotic spindle checkpoint, then inhibition of Mps1 kinase activity should override this and cause dephosphorylation of mitotically phosphorylated proteins. Instead, Rab4a phosphorylation and the amount of MPM2 antigens were the same with or without SP600125, revealing that the effect of juglone on mitotic protein dephosphorylation is not due to the activation/maintenance of the mitotic spindle checkpoint.

During the experiments with SP600125, we uncovered an additional and previously unknown target of juglone that has a function in the orderly progression of the cell cycle. As with tubulin, juglone also caused the disappearance of BubR1 immunoreactivity. BubR1 is an essential kinase of the mitotic checkpoint response and is heavily phosphorylated by Cdk1 and plk1 during mitosis (40). Through interaction with Cdc20, it can negatively regulate the APC/C (46). Tubulin and BubR1 are both cytoplasmic proteins with a high content of cysteine residues whose free SH groups are amenable to alkylation by *p*-benzoquinones. The binding domain of Cdc20 on BubR1 contains 8 Cys residues. It is quite possible that the alkylation of one or more of these SH groups by juglone will also interfere with the normal function of the APC/C degradation machinery.

The abrogated spindle assembly correlated with the modification of SH groups in tubulin that are critical for polymerization into microtubules. Our *in vivo* findings are in agreement with the covalent binding of *p*-benzoquinone derivatives to tubulin *in vitro* (43, 44). Low concentrations of juglone already altered critically cysteines, consistent with the observation that mutation of even a single cysteine in α-tubulin inhibits its polymerization (47). This modification changes the local charge distribution in peptide side chains and can cause conformational alterations that perturb folding and may induce aggregation. A plausible consequence of these alterations is the disappearance of epitopes that are recognized by specific antibodies, as we found for α-tubulin and BubR1. Misfolded BubR1 will be unlikely to assemble properly with Mad2 and Bub3 in the mitotic checkpoint complex, since reduced levels of BubR1 dramatically affect mitotic progression (48, 49). Because BubR1 is a pseudosubstrate inhibitor of Cdc20 (50), it would be expected that juglone interferes with the function of APC/C and pleiotropically perturbs progress into anaphase. Another possibility is that juglone directly inhibits the APC/C. This could mimic the activation of the spindle checkpoint and would prevent the destruction of cyclin B1 even in the absence of an active checkpoint, as we found with the Mps1 inhibitor.

Although juglone exhibited some characteristics of a spindle poison, it did not arrest unsynchronized or presynchronized cells in prometaphase of mitosis. In fact, we found that long term treatment with low juglone concentrations caused the accumulation of cells in S phase and a concomitant decrease of cells with 4 N DNA content. Given the effect of juglone on proteins with such distinct functions as Pin1, α-tubulin, and BubR1, it may also target cell cycle regulators necessary for the S/G_2 and G_2/M transitions. Indeed, it has been reported that juglone (at much higher concentrations than we described in metaphase cells) "freezes" cells in S phase, which was thought to reflect the inhibition of Pin1 (51). The involvement of Pin1 should, however, not be inferred from inhibitor studies with juglone (51, 52), because the effects can be recapitulated in $Pin1^{-/-}$ cells, as we showed. Moreover, the higher concentrations of juglone that were used to inhibit the S/G_2 transition can also induce oxidative stress, DNA damage, and subsequent apoptosis (42, 44). Importantly, we only observed an increased number of cells with sub-G_1 DNA content (Fig. 6*B*) with

TABLE 1
Cellular targets affected by juglone in this study

Process	Cell type	Juglone
		μM
Rab4 dephosphorylation	MEF (CHO)	>0.1 (>2.0)
Tubulin aggregation	MEF (CHO)	>2.0 (>10.0)
Mitotic spindle formation	MEF	>1.0
Cyclin B degradation	MEF	>1.0
Microtubule disruption in interphase cells	MEF (CHO)	>5.0 (>15.0)
BubR1 aggregation	U2OS	>5.0
Apoptosis[a]	MEF	>10.0
Accumulation of cells in S phase[a]	MEF	~5.0
Depletion of cells in G_2/M transition[a]	MEF	~5.0

[a] Effects observed after prolonged (>12-h) treatment with juglone.

juglone concentrations that were significantly higher than required for the inhibition of protein dephosphorylation and spindle formation.

Juglone-induced tubulin modification might evoke additional downstream effects that could correlate with phenotypes in response to alternative strategies for interfering with Pin1 function. Especially, changes in properties like subcellular localization, cell shape, and intracellular transport can be a indirect consequence of disturbed microtubule networks. In summary, we showed that juglone exerts biological effects that can be misinterpreted as a specific phenotype of Pin1 inhibition with respect to its regulation of PP2A-mediated dephosphorylation processes. A summary of the effects of juglone observed in this paper is given in Table 1. More specific Pin1 inhibitors with less side effects are required. Promising candidates are the substituted aryl 1-indanyl ketones (53) and a series of specific D-phospho-Thr-containing peptides (54, 55). Such inhibitors might not only be useful in studying the functional relevance of Pin1 *in vivo*; they could also provide the therapeutic basis to treat pathological conditions in which Pin1 is aberrantly upregulated, such as cancer (8).

Acknowledgments—We thank Prof. Marileen Dogterom for the generous supply of PC-purified bovine brain tubulin and Dr. Giannino del Sal (Laboratorio Nazionale C.I.B. Trieste) for the Pin1$^{-/-}$ cells. We are also grateful to Prof. Rene Medema (Experimental Oncology, University Medical Center Utrecht) for reagents and helpful discussions. Rene M. C. Scriwanek is acknowledged for the preparation of figures.

REFERENCES

1. Schmid, F. X. (2001) *Adv. Protein Chem.* **59,** 243–282
2. Shaw, P. (2007) *EMBO Rep.* **8,** 40–45
3. Fanghanel, J., and Fischer, G. (2004) *Front. Biosci.* **9,** 3453–3478
4. Hennig, L., Christner, C., Kipping, M., Schelbert, B., Rucknagel, K. P., Grabley, S., Kullertz, G., and Fischer, G. (1998) *Biochemistry* **37,** 5953–5960
5. Lu, K. P., and Zhou, X. Z. (2007) *Nat. Rev. Cell Mol. Biol.* **8,** 904–916
6. Yaffe, M. B., Schutkowski, M., Shen, M., Zhou, X. Z., Stukenberg, P. T., Rahfeld, J. U., Xu, J., Kuang, J., Kirschner, M. W., Fischer, G., Cantley, L. C., and Lu, K. P. (1997) *Science* **278,** 1957–1960
7. Shen, M., Stukenberg, P. T., Kirschner, M. W., and Lu, K. P. (1998) *Genes Dev.* **12,** 706–720
8. Yeh, E. S., and Means, A. R. (2007) *Nat. Rev. Cancer* **7,** 381–388
9. Muto, N., Inouye, K., Inada, A., Nakanishi, T., and Tan, L. (1987) *Biochem. Biophys. Res. Commun.* **146,** 487–494
10. Frew, T., Powis, G., Berggren, M., Gallegos, A., Abraham, R. T., Ashendel, C. L., Zalkow, L., Hudson, C., Gruszecka-Kowalik, E., Burgess, E. M., Benedetti-Doctorovich, V., Kerrigan, J. E., Lambropoulos, J., Merriman, R., and Bonjouklian, R. (1995) *Anticancer Drug Des.* **10,** 347–359
11. Varga, Z., Bene, L., Pieri, C., Damjanovich, S., and Gaspar, Jr., R. (1996) *Biochem. Biophys. Res. Commun.* **218,** 828–832
12. Galas, M. C., Dourlen, P., Begard, S., Ando, K., Blum, D., Hamdane, M., and Buee, L. (2006) *J. Biol. Chem.* **281,** 19296–19304
13. Esnault, S., Braun, R. K., Shen, Z. J., Xiang, Z., Heninger, E., Love, R. B., Sandor, M., and Malter, J. S. (2007) *PLoS One* **2,** e226
14. Kesavapany, S., Patel, V., Zheng, Y. L., Pareek, T. K., Bjelogrlic, M., Albers, W., Amin, N., Jaffe, H., Gutkind, J. S., Strong, M. J., Grant, P., and Pant, H. C. (2007) *Mol. Biol. Cell* **18,** 3645–3655
15. Dougherty, M. K., Muller, J., Ritt, D. A., Zhou, M., Zou, X. Z., Copeland, T. D., Conrads, T. P., Veenstra, T. D., Lu, K. P., and Morrison, D. K. (2005) *Mol. Cell* **17,** 215–224
16. Zhou, X. Z., Kops, O., Werner, A., Lu, P. J., Shen, M., Stoller, G., Kullertz, G., Stark, M. A., Fischer, G., and Lu, K. (2000) *Mol. Cell* **6,** 873–883
17. Ma, J., Arnold, H. K., Lilly, M. B., Sears, R. C., and Kraft, A. S. (2007) *Oncogene* **26,** 5145–5153
18. Yeh, E., Cunningham, M., Arnold, H., Chasse, D., Monteith, T., Ivaldi, G., Hahn, W. C., Stukenberg, P. T., Shenolikar, S., Uchida, T., Counter, C. M., Nevins, J. R., Means, A. R., and Sears, R. (2004) *Nature Cell Biol.* **6,** 308–318
19. Albert, A. L., Lavoie, S. B., and Vincent, M. (2004) *BMC Cell Biol.* **5,** 22
20. He, J., Lau, A. G., Yaffe, M. B., and Hall, R. A. (2001) *J. Biol. Chem.* **276,** 41559–41565
21. He, J., Xu, J., Xu, X. X., and Hall, R. A. (2003) *Oncogene* **22,** 4524–4530
22. Bailly, E., Touchot, N., Zahraoui, A., Goud, B., and Bornens, M. (1991) *Nature* **350,** 715–718
23. van der Sluijs, P., Hull, M., Huber, L. A., Male, P., Goud, B., and Mellman, I. (1992) *EMBO J.* **11,** 4379–4389
24. Pfeffer, S. R. (2007) *Annu. Rev. Biochem.* **76,** 629–645
25. Gerez, L., Mohrmann, K., van Raak, M., Jongeneelen, M., Zhou, X. Z., Lu, K. P., and van der Sluijs, P. (2000) *Mol. Biol. Cell* **11,** 2201–2211
26. Fujimori, F., Takahashi, K., Uchida, C., and Uchida, T. (1999) *Biochem. Biophys. Res. Commun.* **265,** 658–663
27. Rippmann, J. F., Hobbie, S., Daiber, C., Guilliard, B., Bauer, M., Birk, J., Nar, H., Garin-Chesa, P., Rettig, W. J., and Schnapp, A. (2000) *Cell Growth Differ.* **11,** 409–416
28. Paulsen, M. T., and Ljungman, M. (2005) *Toxicol. Appl. Pharmacol.* **209,** 1–9
29. Westendorf, J. M., Rao, P. N., and Gerace, L. (1994) *Proc. Natl. Acad. Sci. U. S. A.* **91,** 714–718
30. Van Hoof, C., and Goris, J. (2004) *Cancer Cell* **5,** 105–106
31. Iwamoto, N., Sumi, D., Ishii, T., Uchida, K., Cho, A. K., Froines, J. R., and Kumagai, Y. (2007) *J. Biol. Chem.* **282,** 33396–33404
32. Ryo, A., Nakamura, M., Wulf, G., Liou, Y. C., and Lu, K. P. (2001) *Nat. Cell Biol.* **3,** 793–801
33. Chao, S. H., Greenleaf, A. L., and Price, D. H. (2001) *Nucleic Acids Res.* **29,** 767–773
34. Nogales, E., Grayer, W. S., Khan, I. A., Luduena, R. F., and Downing, K. H. (1995) *Nature* **375,** 424–427
35. Jordan, A., Hadfield, J. A., Lawrence, N. J., and McGown, A. T. (1998) *Med. Res. Rev.* **18,** 259–296
36. O'Connell, C. B., and Khodjakov, A. L. (2007) *J. Cell Sci.* **120,** 1717–1722
37. Musacchio, A., and Salmon, E. D. (2007) *Nat. Rev. Mol. Cell Biol.* **8,** 379–394
38. Abrieu, A., Magnaghi-Jaulin, L., Kahana, J. A., Peter, M., Castro, A., Vigneron, S., Lorca, T., Cleveland, D. W., and Labbé, J. C. (2001) *Cell Microbiol.* **106,** 83–93
39. Schmidt, M., Budirahardja, Y., Klompmaker, R., and Medema, R. H. (2005) *EMBO Rep.* **6,** 867–872
40. Elowe, S., Hümmer, S., Uldschmid, A., Li, X., and Nigg, E. A. (2007) *Genes Dev.* **21,** 2205–2219
41. Bolton, J. L., Trush, M. A., Penning, T. M., Dryhurst, G., and Monks, T. J. (2000) *Chem. Res. Toxicol.* **13,** 135–160
42. Inbaraj, J. J., and Chignell, C. F. (2004) *Chem. Res. Toxicol.* **17,** 55–62
43. Pfeiffer, E., and Metzler, M. (1996) *Chem. Biol. Int.* **102,** 37–53
44. Santa-Maria, I., Smith, M. A., Perry, G., Hernandez, F., Avila, J., and

Moreno, F. J. (2005) *Biochim. Biophys. Acta* **1740,** 472–480
45. DeLuca, J. G., Gall, W. E., Ciferri, C., Cimini, D., Musacchio, A., and Salmon, E. D. (2006) *Cell* **127,** 969–982
46. Reddy, S. K., Rape, M., Margansky, W. A., and Kirschner, M. W. (2007) *Nature* **446,** 921–925
47. Kuriyama, R., and Sakai, H. (1974) *J. Biochem.* (*Tokyo*) **76,** 651–654
48. Chan, G. K. T., Jablonski, S. A., Sudakin, V., Hittle, J. C., and Yen, T. J. (1999) *J. Cell Biol.* **146,** 941–954
49. Kops, G. J. P. L., Foltz, D. R., and Cleveland, D. W. (2004) *Proc. Natl. Acad. Sci. U. S. A.* **101,** 8699–8704
50. Burton, J. L., and Solomon, M. J. (2007) *Genes Dev.* **21,** 655–667
51. Stockwell, B. R., Haggarty, S. J., and Schreiber, S. L. (1999) *Chem. Biol.* **6,** 71–83
52. Kamei, H., Koide, T., Kojima, T., Hashimoto, Y., and Hasegawa, M. (1998) *Cancer Biother. Radiopharm.* **13,** 185–188
53. Daum, S., Erdmann, F., Fischer, G., Feaux de Lacroix, B., Hessamian-Alinejad, A., Houben, S., Frank, W., and Braun, M. (2006) *Angew. Chem. Int. Ed. Engl.* **45,** 7454–7458
54. Wildemann, D., Erdmann, F., Alvarez, B. H., Stoller, G., Zhou, X. Z., Fanghanel, J., Schutkowski, M., Lu, K. P., and Fischer, G. (2006) *J. Med. Chem.* **49,** 2147–2150
55. Zhang, Y., Daum, S., Wildemann, D., Zhou, X. Z., Verdecia, M. A., Bowman, M. E., Lucke, C., Hunter, T., Lu, K. P., Fischer, G., and Noel, J. P. (2007) *ACS Chem. Biol.* **2,** 320–328

Juglone Inactivates Cysteine-rich Proteins Required for Progression through Mitosis

Claudia Fila, Corina Metz and Peter van der Sluijs

J. Biol. Chem. 2008, 283:21714-21724.
doi: 10.1074/jbc.M710264200 originally published online June 6, 2008

SUPPLEMENTARY FIGURES

Figure S1: Validation of Pin1-/- MEFs. Western blot analysis of Pin1 and β-catenin in lysates prepared from wild type (Pin1 +/+) and Pin1-/- MEFs. α-tubulin served as loading control.

Figure S2: High concentrations of juglone disrupt interphase microtubules. **(A)** Interphase CHO cells and Pin1-/- MEFs were grown on coverslips and treated with indicated concentrations of juglone, colchicine or solvent (control) for 2 h. Cells were fixed in 4% paraformaldehyde for 30 min, permeabilized in 0.1% Triton X-100 for 5 min and then labeled for α-tubulin (green) and examined by immunofluorescence microscopy. **(B)** Interphase Pin1-/- MEFs were treated for 12 h with either juglone, colchicine or solvent (control). Cells were lysed and soluble (s) and insoluble (p) fractions were separated by centrifugation and analyzed for α-tubulin by Western blot.

Figure S3: Juglone does not arrest pre-synchronized cells in mitosis. CHO cells were either untreated (1), synchronized with thymidine at the G1/S-phase boundary (2), were then released from the block into S-phase and mitosis (3), and treated with either nocodazole (4) or 5 μM juglone (5) for 5 h. **(A)** Cells were lysed and MPM2 antigens, phospho-rab4a and tubulin were assayed by Western blot. **(B)** Cells were fixed in 70% ice-cold ethanol, treated with RNAse, incubated in propidium iodide and analyzed by flow cytometry using a 488 nm-laser. The histograms were used to quantitate the fraction of cells in G1, S-phase, and G2/M-phase (table).

Figure S4: Juglone inhhibits mitotic exit. **(A)** Pin1-/- MEFs were released from mitotic arrest by removal of nocodazole (noc) and re-seeded on coverslips. Cells were incubated with 1 μM juglone and fixed at indicated times after noc washout. Cells were labeled for α-tubulin (green), stained for DNA (blue) and examined by fluorescence microscopy. White arrow heads indicate zoom-in image of cells shown in Fig. 7A. Numbers indicate the mitotic index.

Figure S1

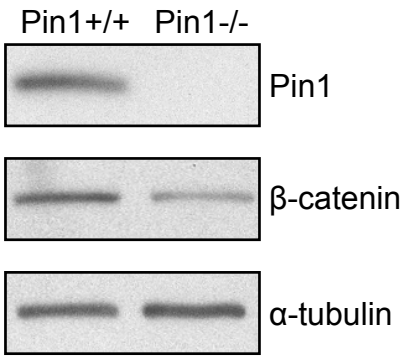

Figure S2

A

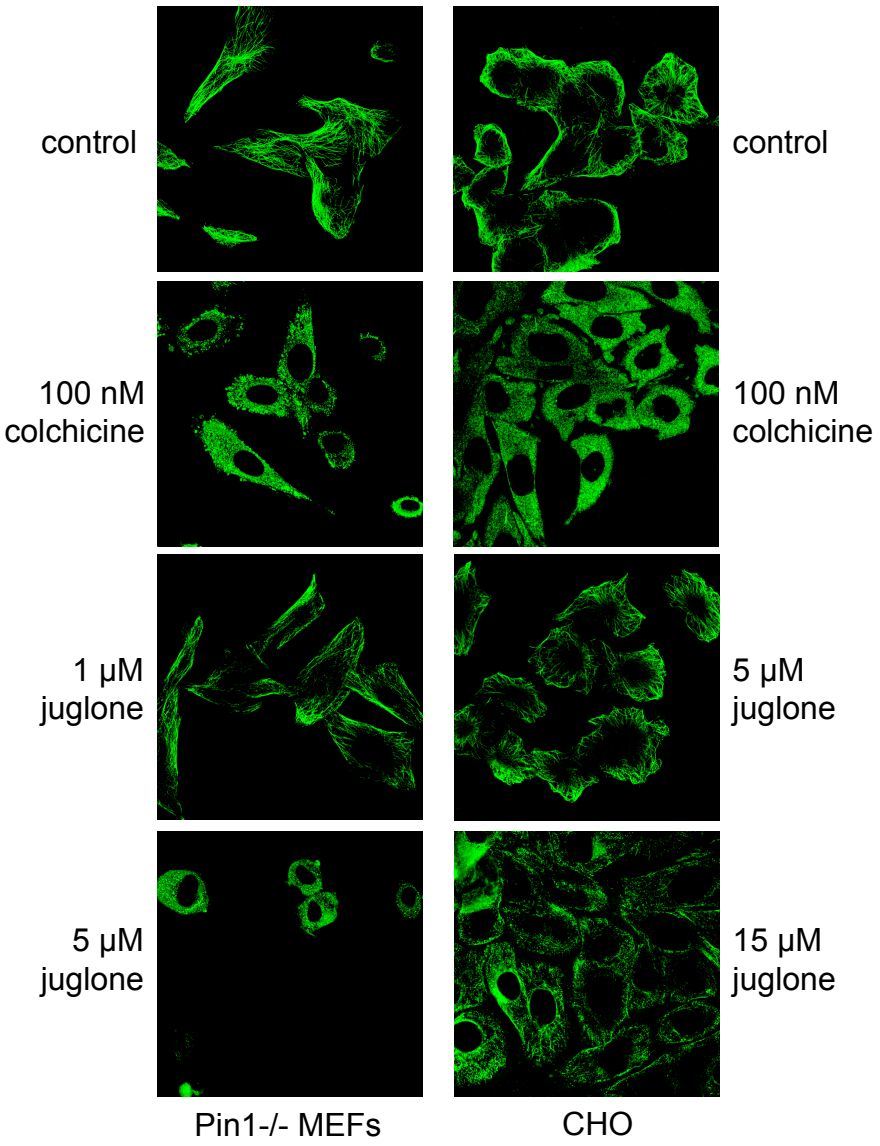
control
control
100 nM colchicine
100 nM colchicine
1 μM juglone
5 μM juglone
5 μM juglone
15 μM juglone
Pin1-/- MEFs
CHO

B

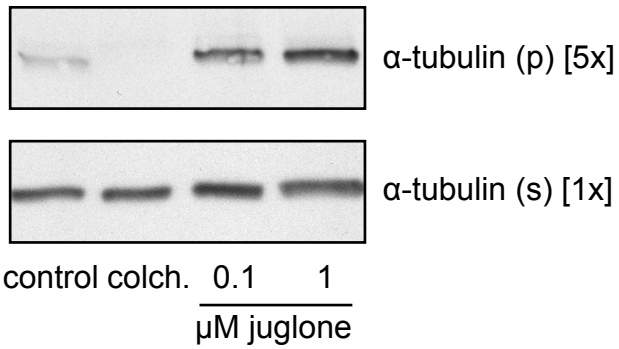
α-tubulin (p) [5x]
α-tubulin (s) [1x]
control colch. 0.1 1
μM juglone

Figure S3

A

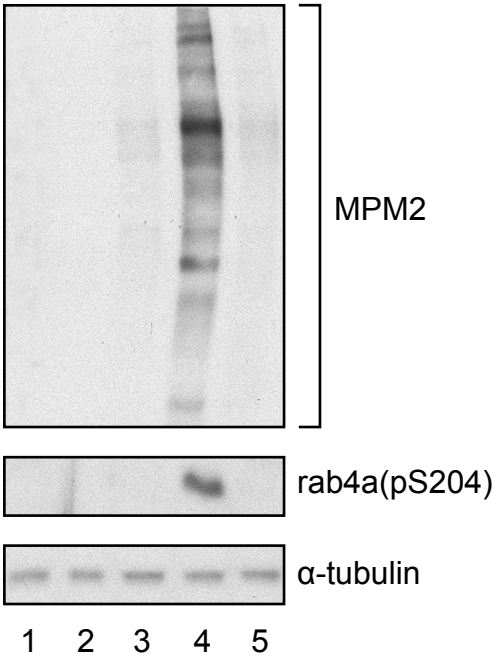

B

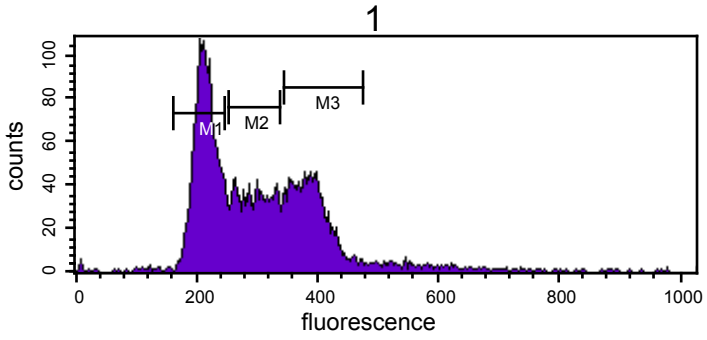

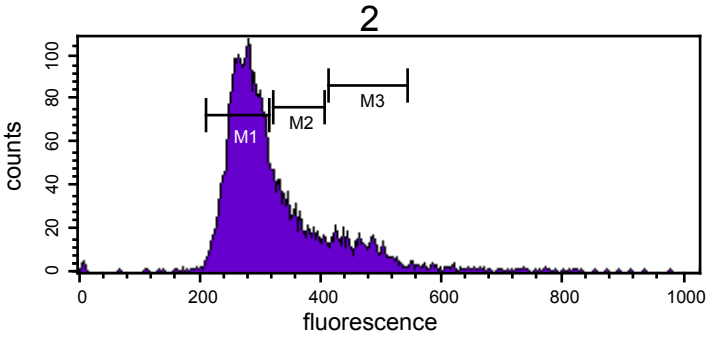

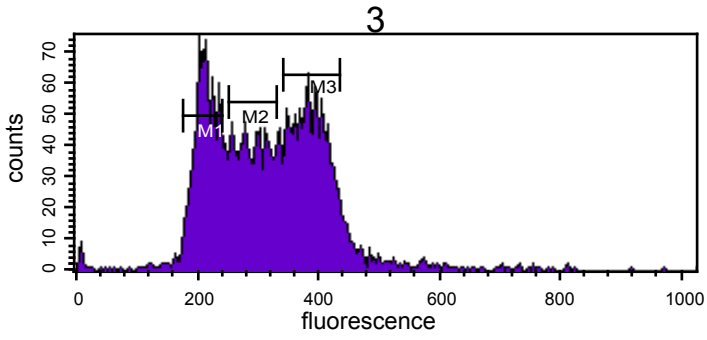

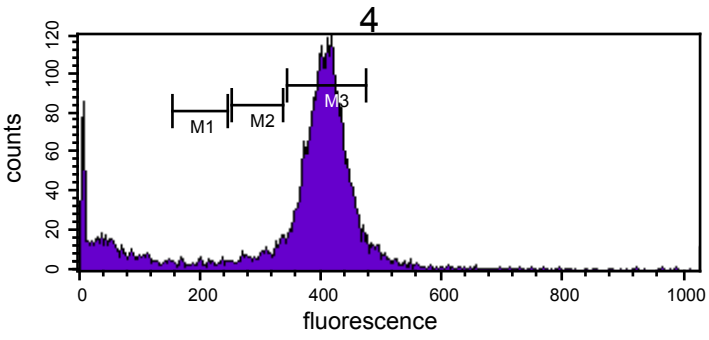

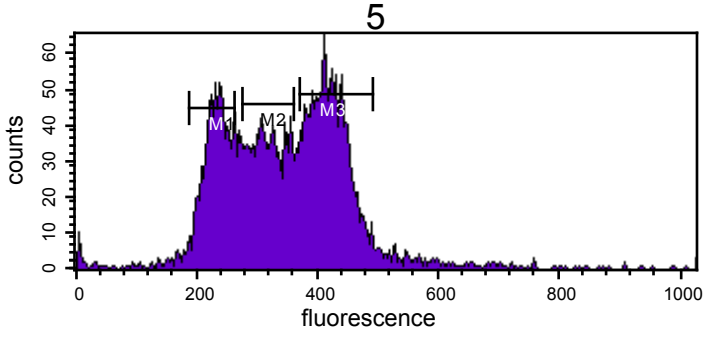

		M1	M2	M3
		G1	S	G2/M
cells (%)	1	39.95	24.71	28.25
	2	65.58	18.21	10.98
	3	28.19	27.89	37.11
	4	2.45	5.73	72.38
	5	22.83	26.60	39.55

Figure S4

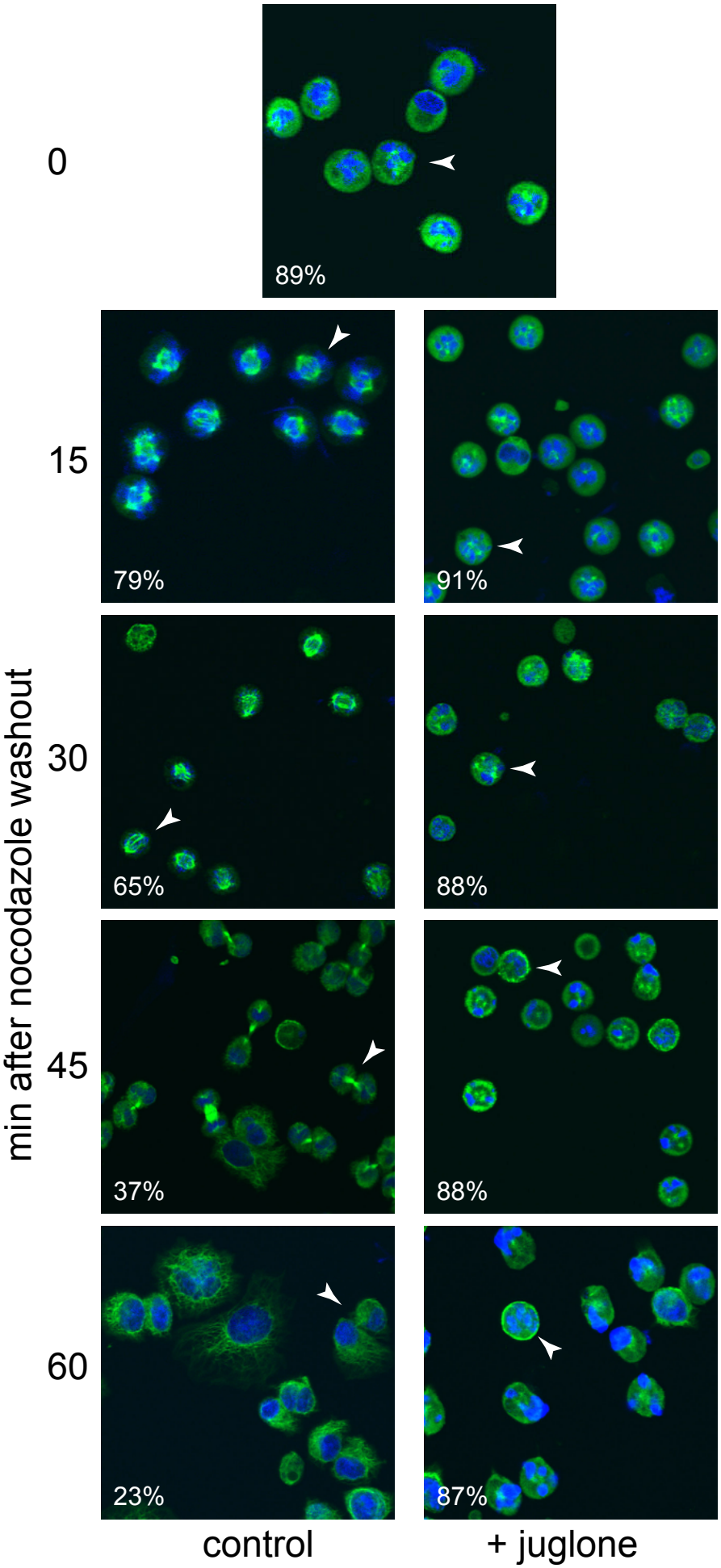
0
89%
15
79%
91%
30
65%
88%
45
37%
88%
60
23%
87%
min after nocodazole washout
control
+ juglone